



Interfacial Processes in EES Systems Advanced Diagnostics

Robert KostECKi

Lawrence Berkeley National Laboratory

Berkeley, California 94720

May 16, 2013

Project ID# ES085

This presentation does not contain any proprietary, confidential, or otherwise restricted information

Overview

Timeline

- PI participated in the BATT Program since 1999
- This project was recompleted in FY12 and renewed in FY13
- Task #1 started on Sept. 1, 2011
80% completed
- Task #2 initiated on April 1, 2012
60% completed

Barriers Addressed

- Low Li-ion battery energy density, and calendar/cycle lifetimes for PHV and EV applications
- Inadequate cell/electrode impedance that limits power and affects system safety

Budget

- FY13 funding \$500K
- FY12 funding \$520K
- FY11 funding \$520K
- FY10 funding \$520K
- FY09 funding \$520K
- FY08 funding \$485K

Partners

- BATT Cathode and Anode Task Groups
 - ANL, LBNL, SUNY, UP, HQ and UU
 - G. Chen, J. Kerr, J. Cabana,,
M. Doeff, K. Persson (LBNL)
- V. Srinivasan and M. Foure (LBNL) are BATT program lead and program manger, respectively

Objectives

- Establish direct correlations between electrochemical performance, interfacial phenomena, surface chemistry, morphology, topology and degradation mechanisms of BATT baseline electrodes
- Evaluate and improve the capacity and cycle life of Li-ion intermetallic anodes and high-voltage cathodes:
 - Determine the mechanism and role of interfacial processes in high-energy Li-ion cells; determine physico-chemical properties and functionality of electrode interfacial layers e.g., SEI, including chemical composition, morphology and topology of ionic/electronic conductivity
 - Investigate electrocatalytic behavior of Li-ion electrodes in organic electrolytes as the function of surface composition and crystalline orientation
 - Provide remedies to interface instability e.g., artificial surface layers (e.g., ALD) and/or structures, novel electrode architecture, electrolyte additives, co-intercalation of secondary metals/ions etc.
 - Characterize active material/electrode/cell degradation modes, improve long-term stability of high-energy Li-ion systems
- Develop, adapt and employ new experimental techniques and methodologies to study EES materials and systems

Milestones

- Characterize surface phenomena and bulk phenomena in high-voltage composite cathodes in collaboration with the BATT Cathode Group (September 2012)
 - Accomplished on time. Determined that decomposition of linear carbonates is responsible for the formation of a surface layer on Li-cathodes at elevated potentials
- Adapt near-field IR and Raman spectroscopy to characterize battery materials (September 2012)
 - Accomplished on time. Near-field IR microscopy was applied for the first time to study the lithiation/delithiation behavior of Li-ion materials
- Resolve SEI layer chemistry of Si model single crystal anodes in collaboration with the BATT Anode Group (July 2013)
 - Work in progress ~ 50% completed
- Characterize interfacial phenomena in high-voltage composite cathodes in collaboration with the BATT Cathode Group (September 2013)
 - Work in progress ~ 60% completed
- Incorporate an *in situ* electrochemical cell into existing ultrafast laser beam delivery/automated translation stage/spectrometer LIBS system
 - Work in progress ~ 40% completed

Interfacial Activity of High-Voltages Cathodes

Approach

- Apply *in situ* and *ex situ* Raman, fluorescence, FTIR spectroscopy and standard electrochemical techniques to characterize interfacial phenomena on $\text{LiNi}_{0.5}\text{Mn}_{1.5}\text{O}_4$ during charge/discharge
 - Perform *in situ* measurements on composite cathodes and model single particle electrodes
 - Carry out preliminary spectroscopic measurements on model $\text{LiNi}_{0.5}\text{Mn}_{1.5}\text{O}_4$ single crystals with preferred surface crystalline orientation

Accomplishments

- Determined the mechanism of interfacial processes on $\text{LiNi}_{0.5}\text{Mn}_{1.5}\text{O}_4$
 - Inorganic and organic fluorescent electrolyte decomposition products form at the cathode and anode
 - Mn and/or Ni dissolution leads to formation of soluble fluorescent species, which diffuse toward the anode and interfere with the anode (SEI Mn/Ni poisoning?)
 - Insoluble electrolyte decomposition products form electronic and ionic barriers in composite cathodes and contribute to the impedance rise in Li-ion cells

In situ Spectroscopy of $\text{LiNi}_{0.5}\text{Mn}_{1.5}\text{O}_4$ Single Particle

Objective: probe reactivity of the cathode active material/electrolyte interface

Raman spectroscopy – monitor local electrode structure

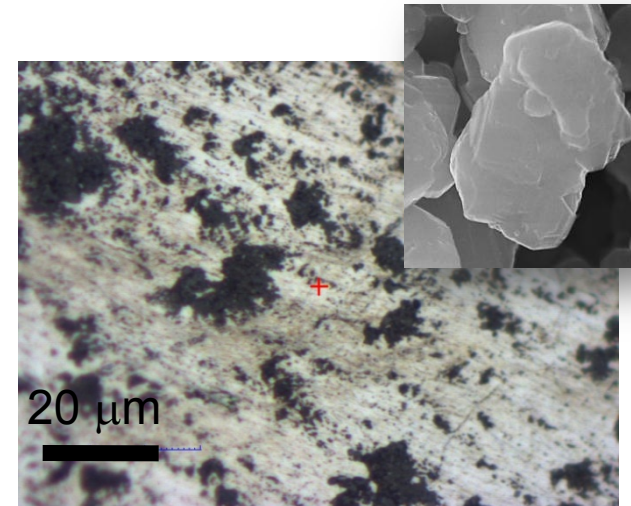
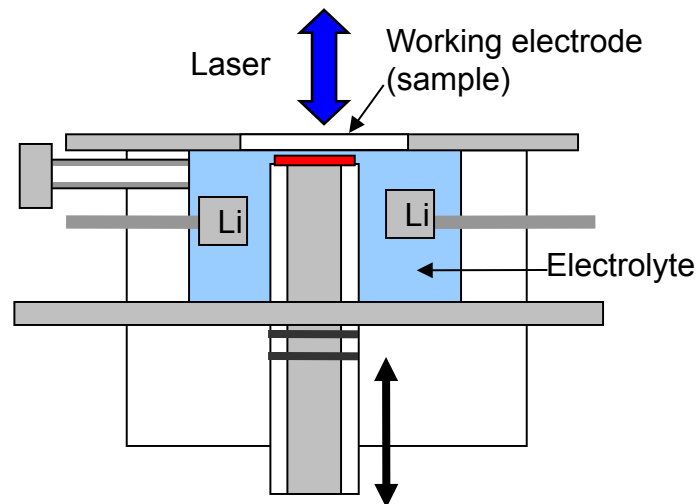
- A common problem – presence of a large fluorescence background

Fluorescence spectroscopy – new tool to probe interfacial reactivity

- Fluorescent species originate from side reactions
- Quantitative and qualitative analysis of electrode/electrolyte decomposition products at the electrode surface

In situ spectro-electrochemical cell
(used with confocal Raman microscope)

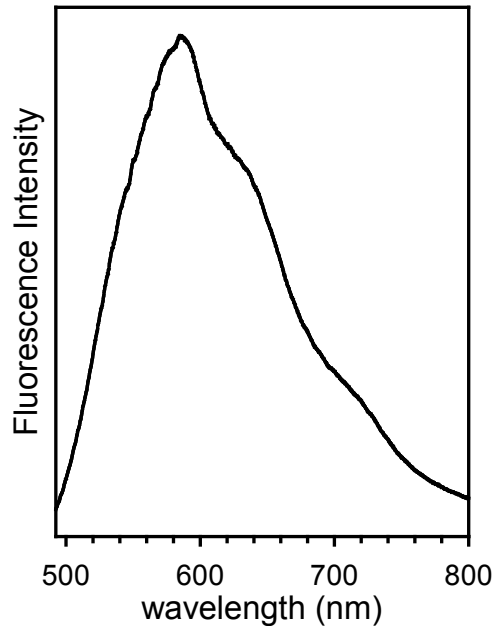
$\text{LiNi}_{0.5}\text{Mn}_{1.5}\text{O}_4$ powder on Al
(carbon & binder free)



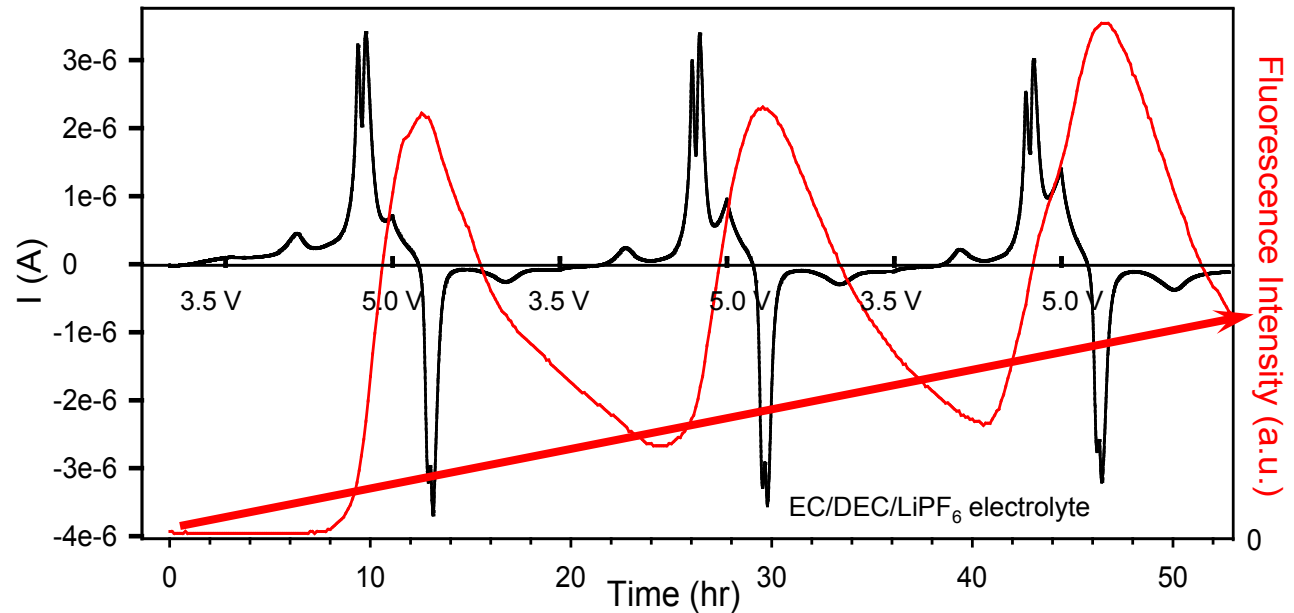
In situ Fluorescence Spectroscopy of $\text{LiNi}_{0.5}\text{Mn}_{1.5}\text{O}_4$ Single Particle

Strong fluorescence is a common phenomenon observed in situ and ex situ in cycled high-voltage cathodes. It originates from inorganic species that form during electrolyte decomposition. Fluorescence spectroscopy can be used to probe the composition and dynamics of surface film (re)formation during charge/discharge cycling.

Fluorescence spectrum
(Excitation $\lambda = 488$ nm)

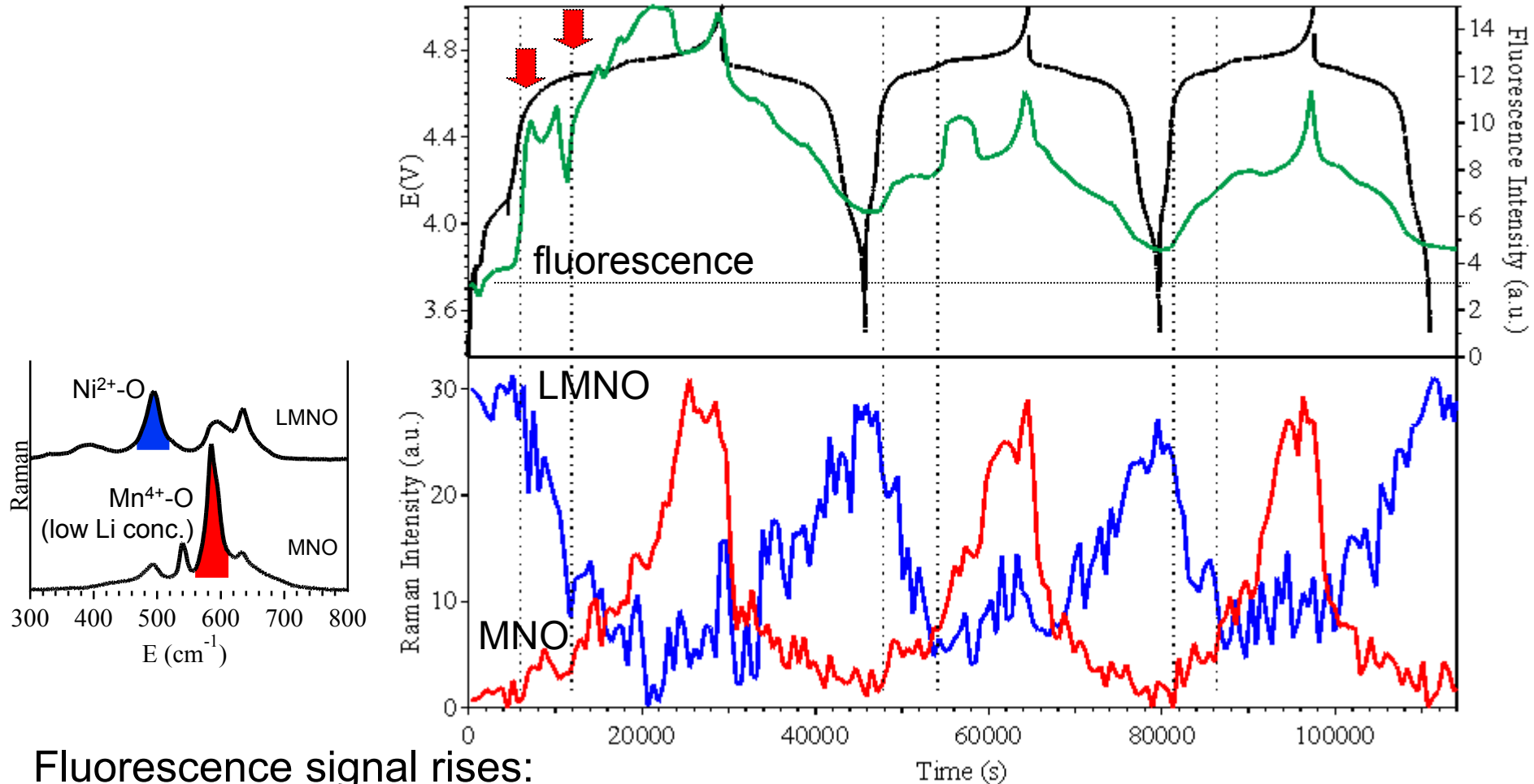


***In situ* Fluorescence Spectroscopy**



- Electrolyte oxidation products form on the surface of LNMO during charging and slowly disappear from the electrode surface during discharge
- Fluorescent decomposition products also tend to accumulate on the surface of LNMO during cycling

In situ Fluorescence and Raman Spectroscopy of $\text{LiNi}_{0.5}\text{Mn}_{1.5}\text{O}_4$ Single Particle



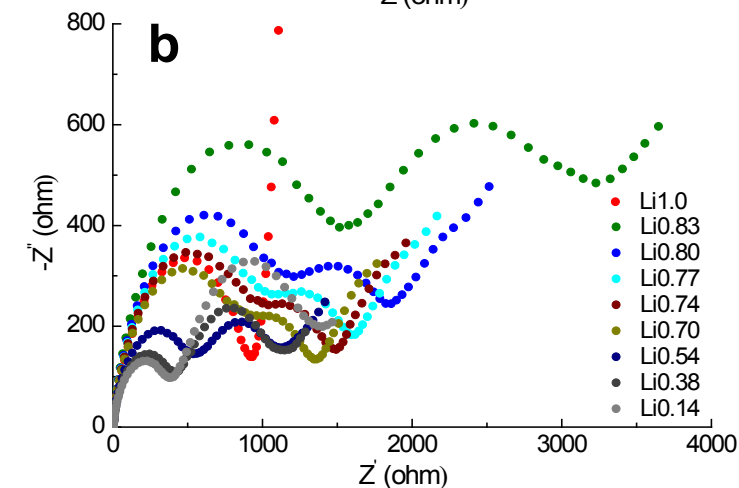
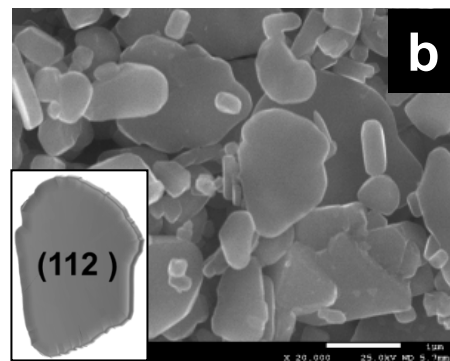
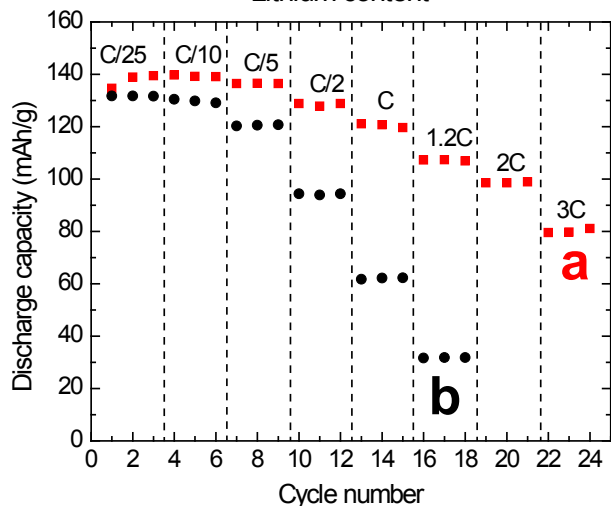
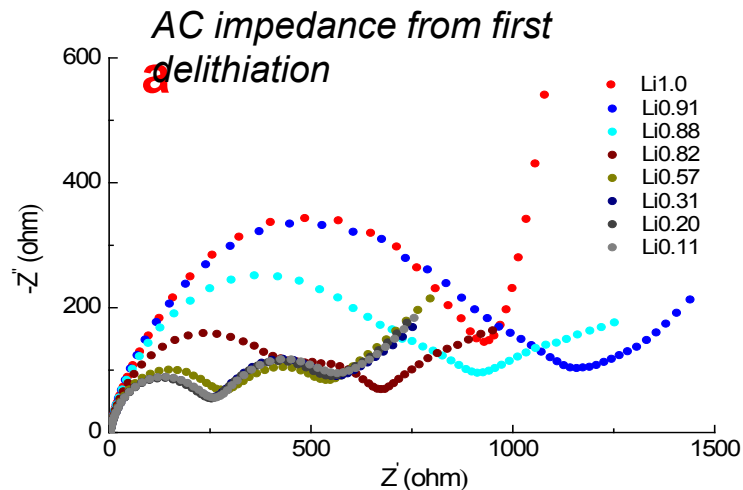
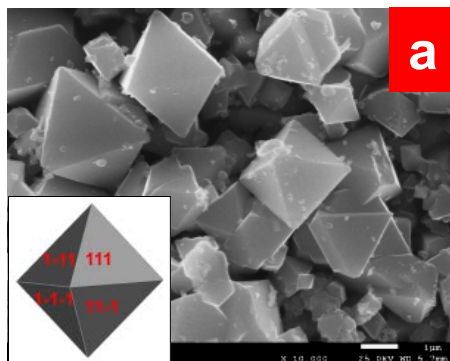
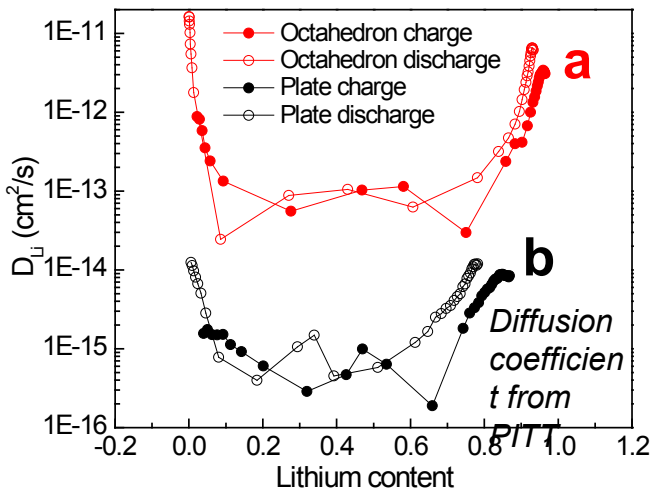
Fluorescence signal rises:

- at the beginning of Ni²⁺ oxidation (Ni²⁺-O stretch decreases)
- with Mn-O stretch at 585 cm⁻¹ (close to Ni^{3+/4+} oxidation threshold)

Electrolyte decomposition at high potentials occurs at Niⁿ⁺ sites

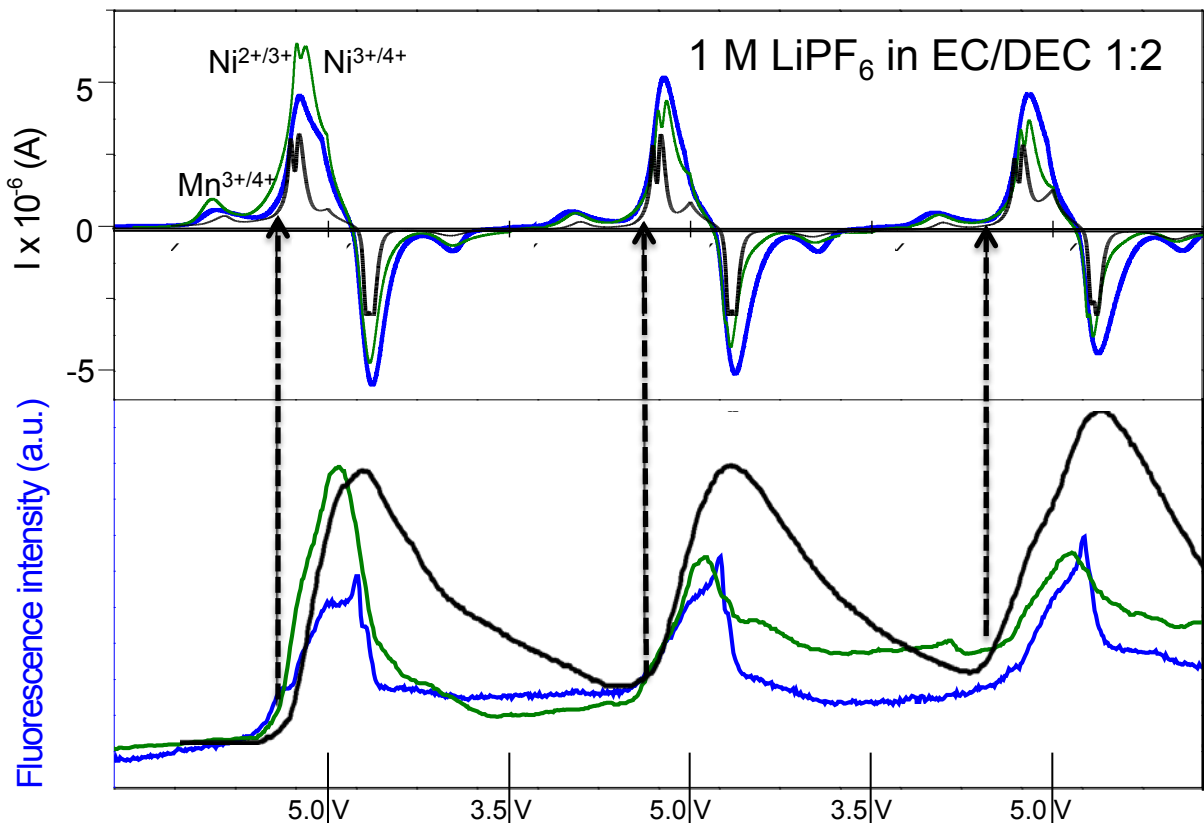
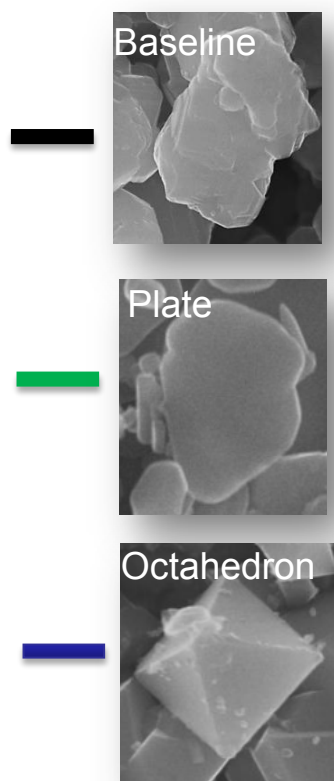
Single Crystal Diagnostics – $\text{LiMn}_{1.5}\text{Ni}_{0.5}\text{O}_4$ Spinel

G. Chen, LBNL



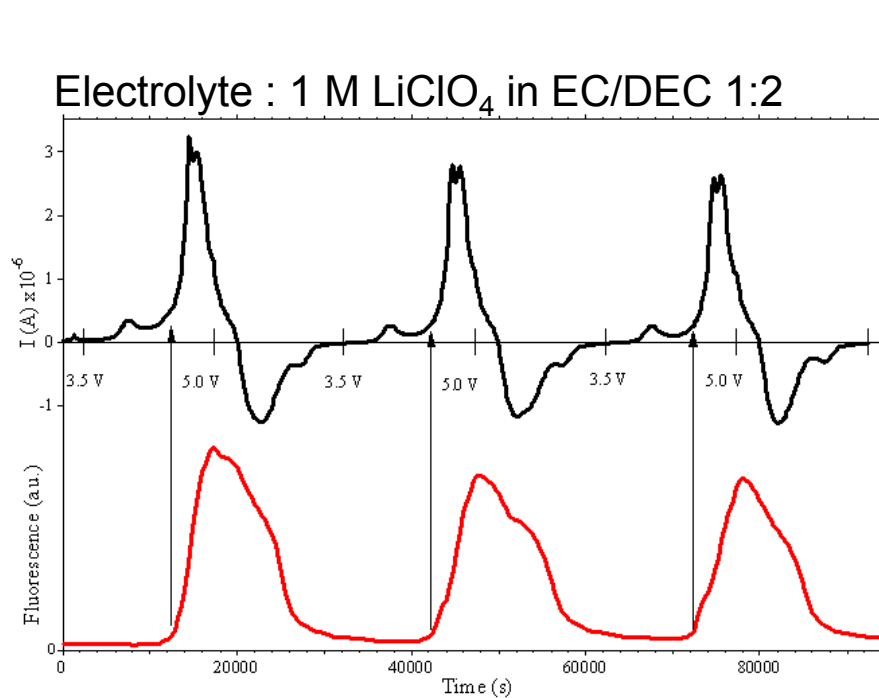
Particle morphology and surface crystalline orientation are critical for superior rate capability and interfacial stability – higher rate and lower reactivity on (111) surface facets

Single Crystal Diagnostics – $\text{LiMn}_{1.5}\text{Ni}_{0.5}\text{O}_4$ Spinel

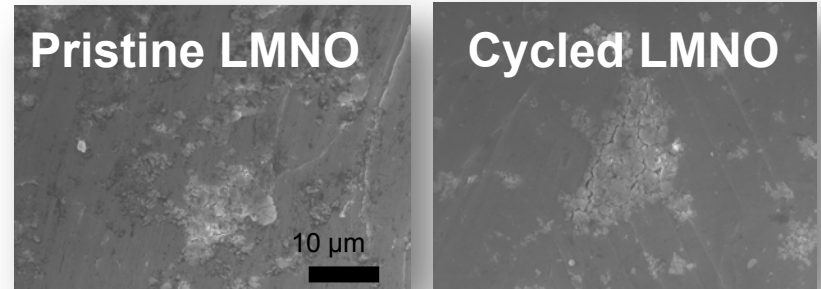


- The rate of electrolyte decomposition varies strongly with the crystalline orientation of LMNO surface and the electrode potential
- Electrolyte oxidation products on LMNO platelets tend to passivate the active material better than octahedrons during the initial charge/discharge cycles

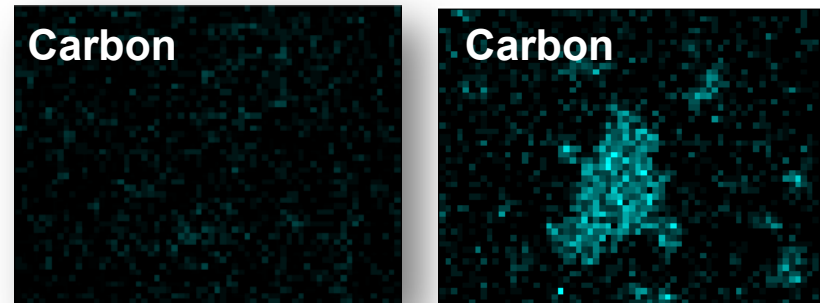
Origins of Fluorescence Compounds in High-Energy Li-ion Systems



SEM



EDX



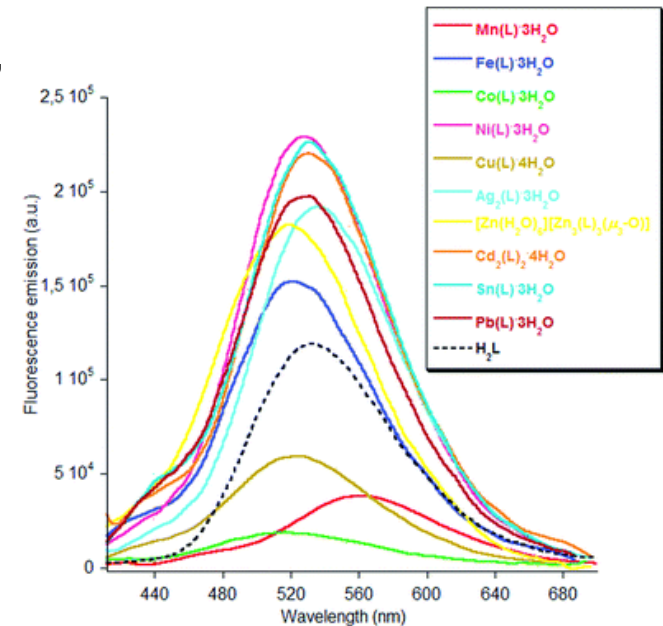
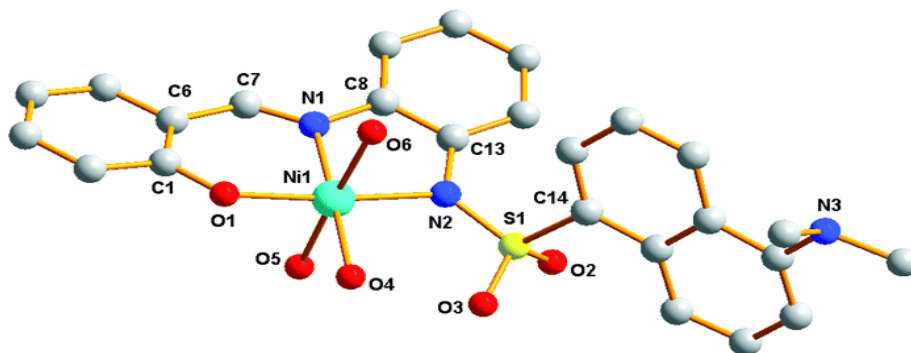
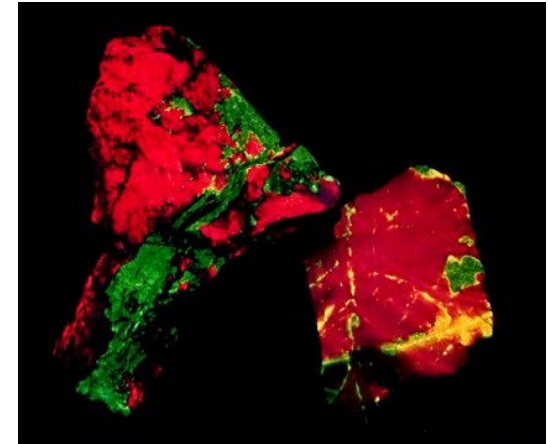
- Strong fluorescence signal from LiNi_{0.5}Mn_{1.5}O₄ is also observed in 1M LiClO₄, EC:DEC electrolyte
- Carbonaceous decomposition products accumulate on LMNO during cycling

Fluorescence compounds originate from oxidation of organic carbonate solvent(s)

Origins of Fluorescence Compounds in Li-ion Systems

Several inorganic/organic compounds exhibit fluorescence:

- Calcite and silicates with Mn^{2+} impurities. Charge transfer between Ca^{2+} and Mn^{2+} stimulates photoluminescence
- Transition metal compounds with a trace amount of dopants, point defects and/or dislocations ($MeP_xO_yF_z$)
- Lithium fluoroalkylphosphate based composite polymer electrolytes (PVdF–HFP) doped with with nanosized SiO_2 displays photoluminescence
- Metallorganic complexes display photoluminescence e.g., $[Me(L)(H_2O)_3] \cdot H_2O \cdot (CH_2CH_3)_2O$
- Metal ions: Li^+ , $Mn^{2+/3+/4+}$ and $Ni^{2+/3+/4+}$; ligands: HMW oligomers (oxidation products of organic carbonates)



http://disc.sci.gsfc.nasa.gov/education-and-outreach/additional/science-focus/ocean-color/science_focus.shtml/fluorescence.shtml

V. Aravindan and P. Vickraman, *Materials Chemistry and Physics*, **115**, 251 (2009)

M. J. Romero, R. Pedrido, A. M. Gonzalez-Noya, M. Maneiro, M. I. Fernandez-Garcia, G. Zaragoza and M. R. Bermejo, *Dalton Transactions*, **41**, 10832 (2012))

Summary I

- Inorganic and organic fluorescent electrolyte decomposition products form at the cathode and dissolve in the electrolyte
 - Fluorescence rise correlates with the beginning of the Ni²⁺ oxidation
 - Ni and possibly Mn ions constitute fluorescence centers in fluorescence compounds formed on LMNO positive electrodes
 - Solvent oxidation at LMNO leads to formation of soluble fluorescent species, which diffuse toward the anode and interfere with the SEI (Mn/Ni poisoning?)
 - Adequate particle morphology is critical in achieving optimal rate capability and stability of the high-voltage LMNO spinel
- Insoluble electrolyte decomposition products form electronic and ionic barriers in composite cathodes and contribute to the impedance rise in Li-ion cells
- Electrolyte additives, surface coatings could be effective strategies to reduce surface reactivity of high-voltage cathodes

see ES033 poster

Sensing Electrode/Electrolyte Interfaces with Near-Field Optical Probes

Approach

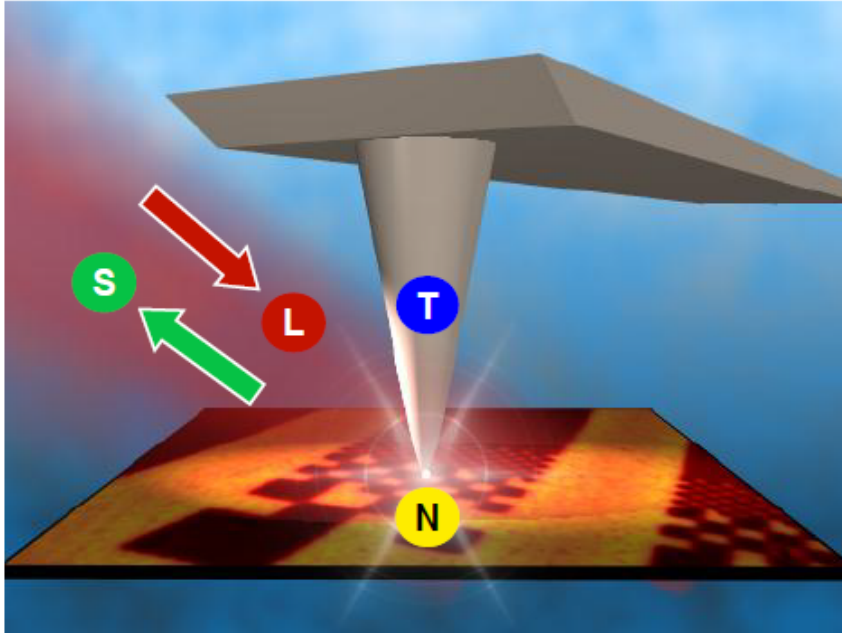
- Develop and employ novel *in situ* and *ex situ* advanced spectroscopy and imaging probes to characterize structure, composition and function of electrochemical interfaces in EES systems
 - Resolve signal from individual building blocks of composite electrodes and surface films and determine their roles and function
 - Assess impact of these fundamental phenomena on the electrochemical performance and lifetime of Li-ion cells

Accomplishments

- Pioneered the use of near-field IR spectroscopy and microscopy to study electrochemical interfaces in Li-ion systems
 - New technique and experimental methodology was developed under the BES-funded NECCES (Energy Frontier Research Center)
 - Preliminary measurements carried out on a model Sn-foil anode revealed non-uniform distribution of electrolyte decomposition products at nanometer scale

Near-Field IR Spectroscopy and Microscopy

Simultaneous measurement of mechanical topography and optical near-fields

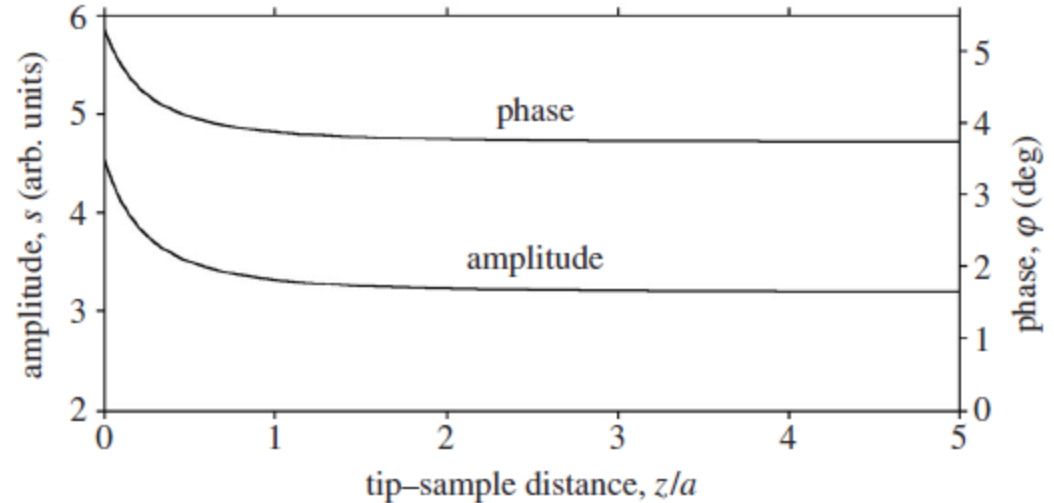
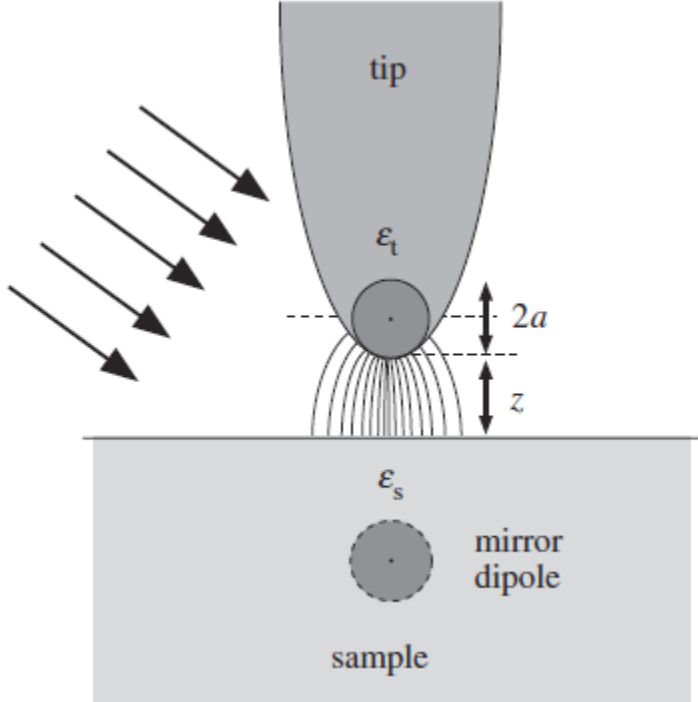


- ✘ A focused laser-beam **L** illuminates a commercial AFM tip **T**
- ✘ The tip generates a nano-focus **N** about the size of the tip-radius of 10 nm (Lightning Rod Effect)
- ✘ The near-field interaction between the tip and the sample modifies the elastically-scattered light **S**
- ✘ By scanning the sample surface with the tip, an optical image with 10nm spatial resolution is created

Characterize and monitor dynamics of bulk and interfacial basic phenomena

- Very high surface sensitivity and discrimination against species in solution
- Nanometer scale (<50nm) *in situ* imaging with high spectral and temporal resolving power

Theoretical Background

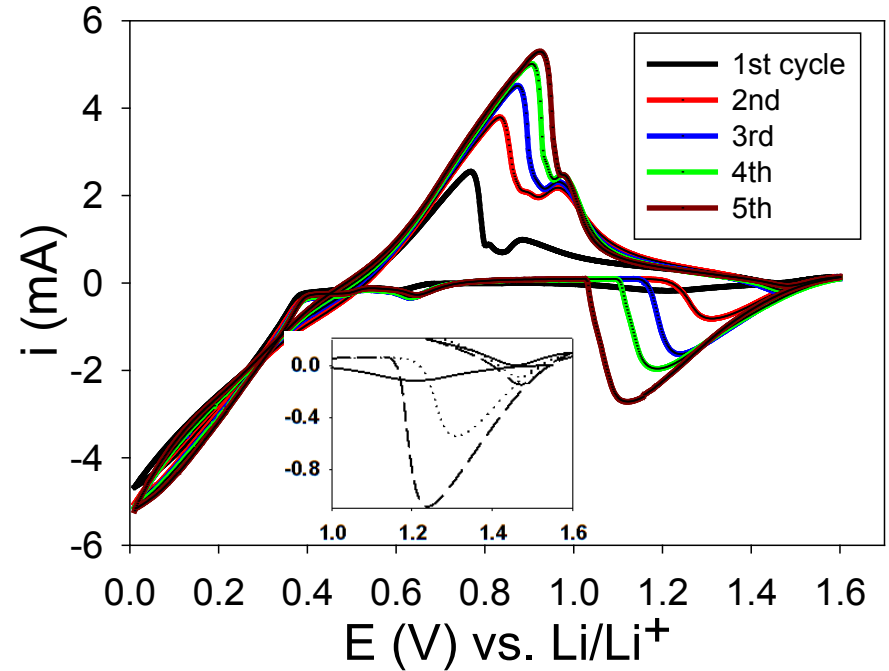
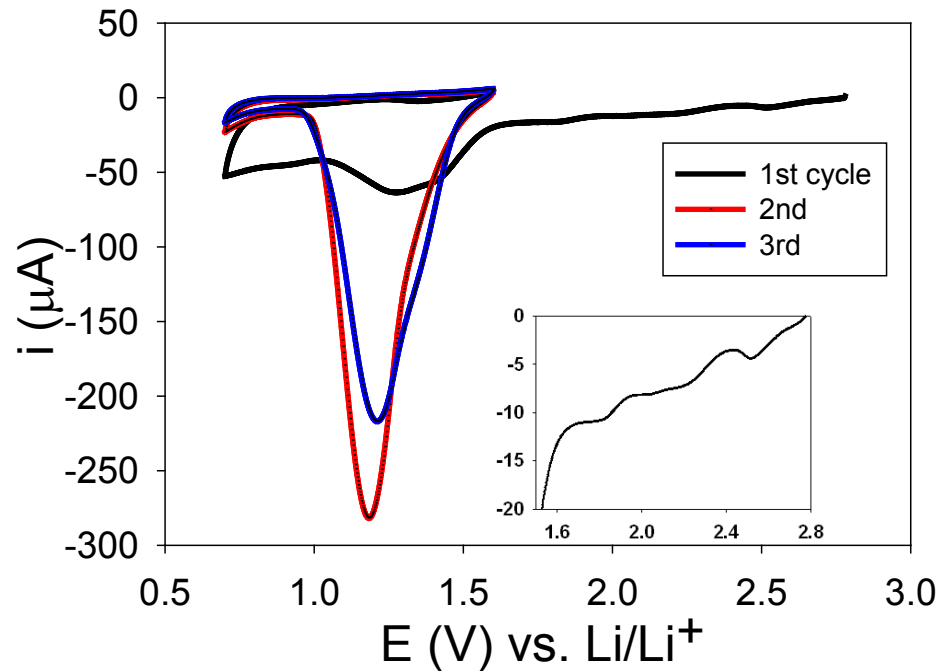


[1] Keilmann, Hillebrand, Phil. Trans. Royal Society 362(1817):787–805 (2004)

- The nonlinear dependence $\alpha_{\text{eff}}(z)$ is used to eliminate unwanted ‘background’ scattering which generally dominates the detected signal.
- The focused laser beam illuminates a greater part of the tip shaft which typically extends $10 \mu\text{m}$ from the cantilever, and also the sample.
- A small portion of the incident light can be assumed to reach the gap region and to contribute to the probing near-field.

Cyclic Voltammetry of Sn-foil Anodes

Sn-foil anode in 1M LiPF₆, EC:DEC (1:2)



- Irreversible electrolyte reduction peaks appear at 1.45 and 1.2 V
 - The peak at 1.45 V remains unchanged whereas the intensity of the peak at 1.2 V quadruples during the two following cycles.
- Large volumetric changes of Sn crystallites lead to Sn particle decrepitation and continuous regeneration of a fresh tin surface and SEI reformation

Near-Field IR Spectroscopy: Imaging of SEI on a Polycrystalline Sn Electrode

Topography

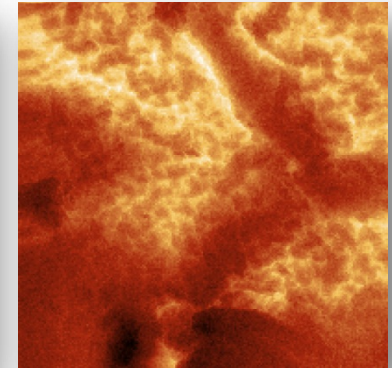
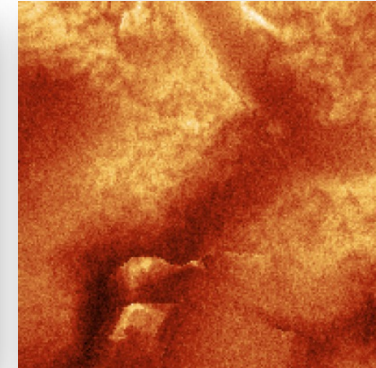
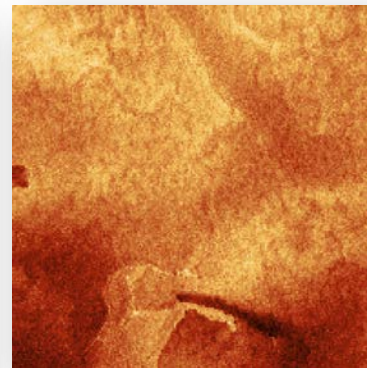
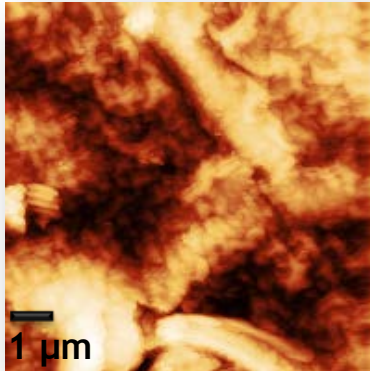
Near-Field IR Images at Single Wavelengths

1087 cm^{-1}

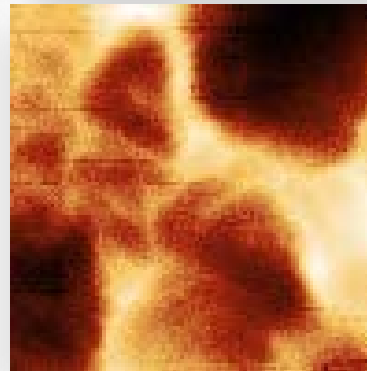
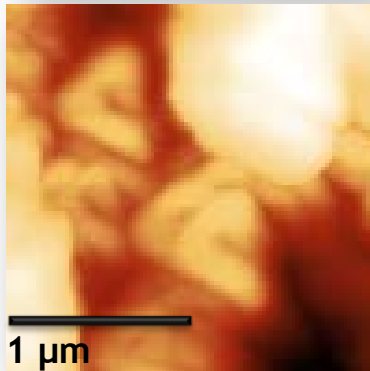
1042 cm^{-1}

1000 cm^{-1}

Sn at
0.8 V



Li_xSn at
0.1 V



- Topography and IR chemical composition images were recorded in a single measurement
 - Structural and chemical information in a single step at 20 nm resolution
- Changes in N-F signal intensity and contrast as the function of the incident IR wavelength represents variations of SEI layer chemical composition

Summary II

- Preliminary *ex situ* near-field IR imaging of a SEI layer on Sn-foil model electrode was successfully carried out.
 - Near-Field IR images reveal chemical complexity of the SEI layer and its functionality at nanometer level
- These new experimental results are in concert with earlier far-field spectroscopy observations and provide new insight into the mechanism of interfacial processes on intermetallic anodes
- Need to work with model samples of similar dimensions of functional electrode materials in EES

Near-field optical techniques constitute a class of emerging analytical tools with an unprecedented analytical capabilities toward electrical energy materials and systems

“With this underpinning knowledge, wholly new concepts in materials design can be developed for producing materials that are capable of storing higher energy densities and have long cycle lifetimes”

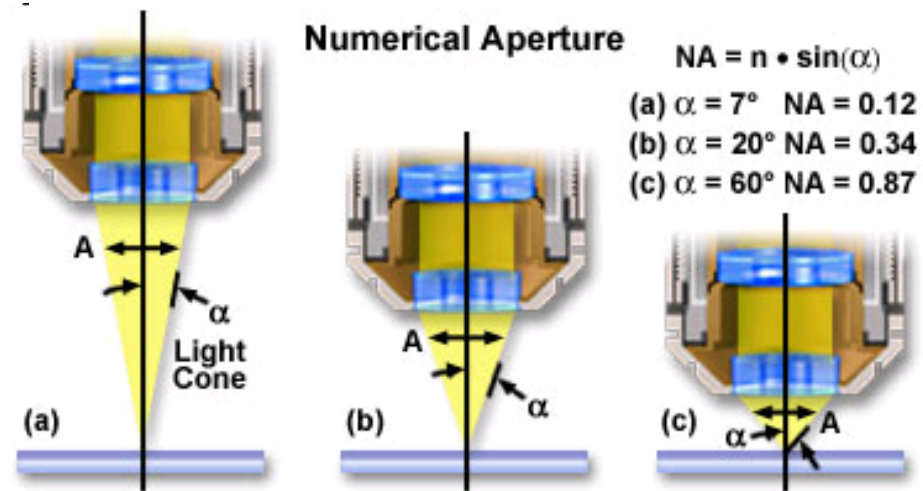
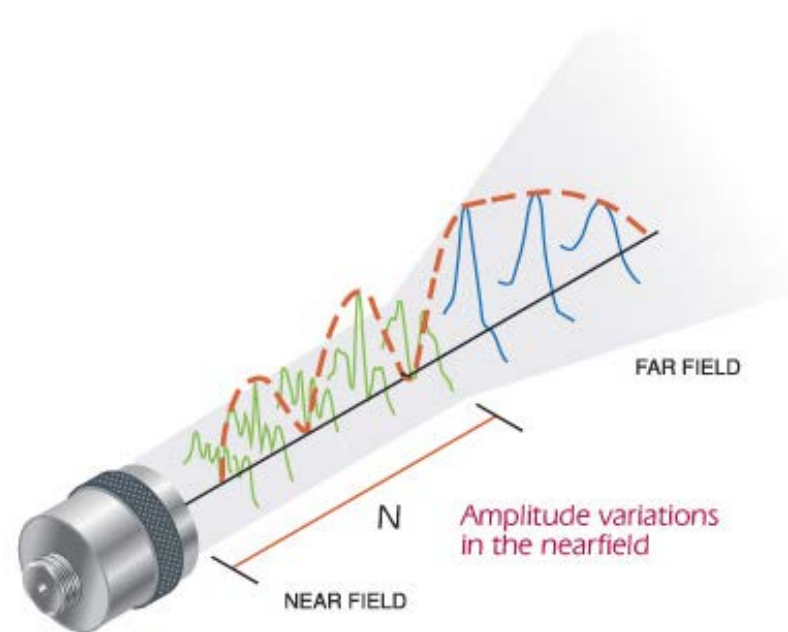
Future Work

- Develop and apply novel innovative experimental methodologies to study and understand the basic function and mechanism of operation of materials, composite electrodes, and Li-ion battery systems for PHEV and EV applications.
- Apply novel far- and near-field optical multifunctional probes to obtain detailed insight into the dynamic behavior of molecules, atoms, and electrons at electrode/electrolyte interfaces of intermetallic anodes (Si) and high voltage Ni/Mn-based materials at a spatial resolution that corresponds to the size of basic chemical or structural building blocks.
- Unveil the structure and reactivity at hidden or buried interfaces and interphases that determine battery performance and failure modes.
- Understanding of the underlying principles that govern these phenomena is inextricably linked with successful implementation of high energy density materials such as Si and high voltage cathodes in Li-ion cells for PHEVs and EVs.
- Cooperate with the BATT Task Groups "SEI on Alloys", "High-Voltage Cathodes" and industrial partners (3M, Dow Chemical) to investigate the effect of material structure, morphology on formation of the SEI layer

Technical backup slides

Far-Field vs. Near-Field Spectroscopy/Imaging

- Region extending farther than 2 wavelengths away from the source is called the *Far-Field*.
 - Relationship between the electric field component E and the magnetic component H is that characteristic of any freely propagating wave, where E is equal to H at any point in space
- Region located less than one wavelength from the source is called the *Near-Field*
 - Relationship between E and H becomes very complex, either field component (E or H) may dominate at any point

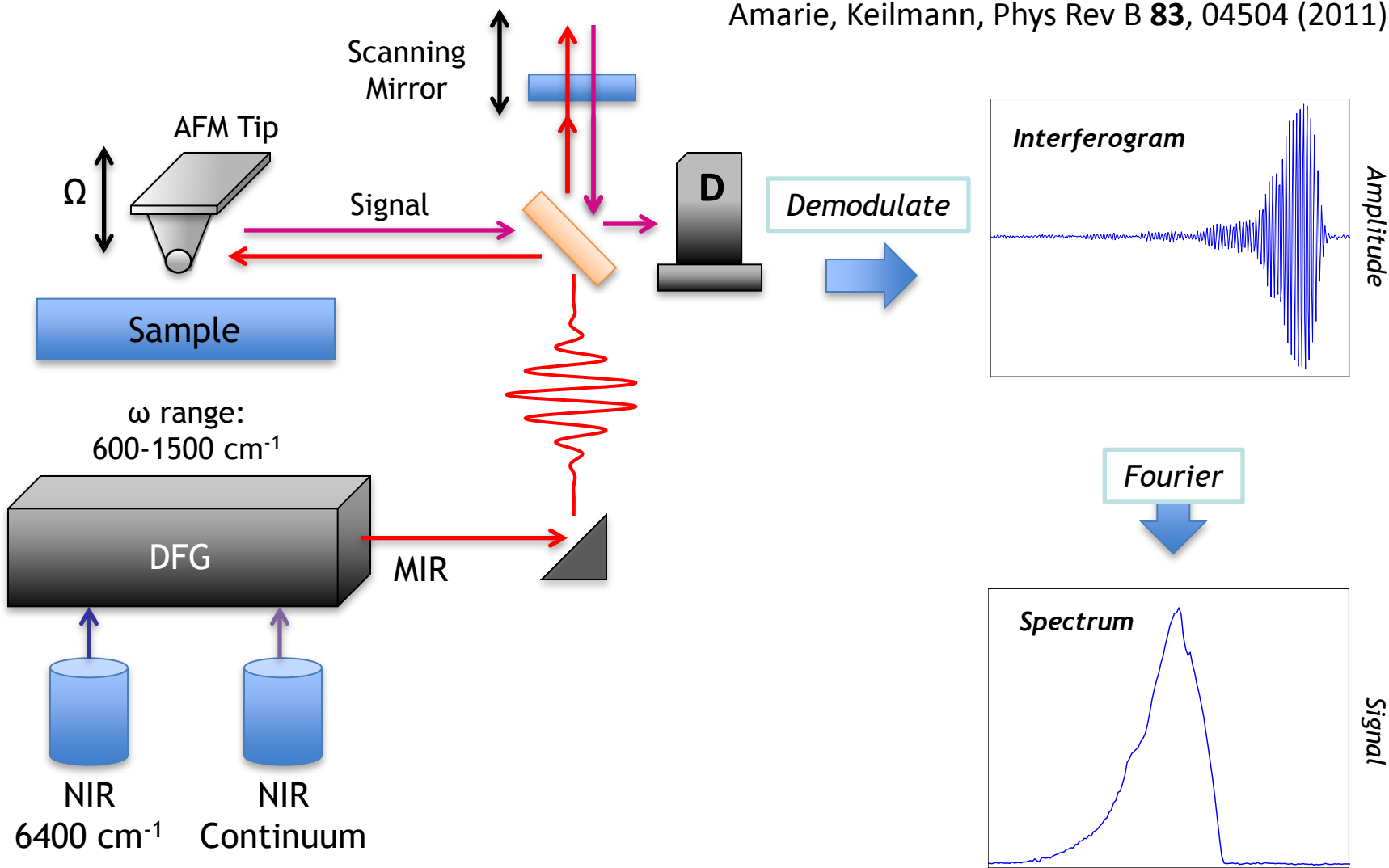


Diffraction limit:

$$d = \frac{0.61 \cdot \lambda}{NA}$$

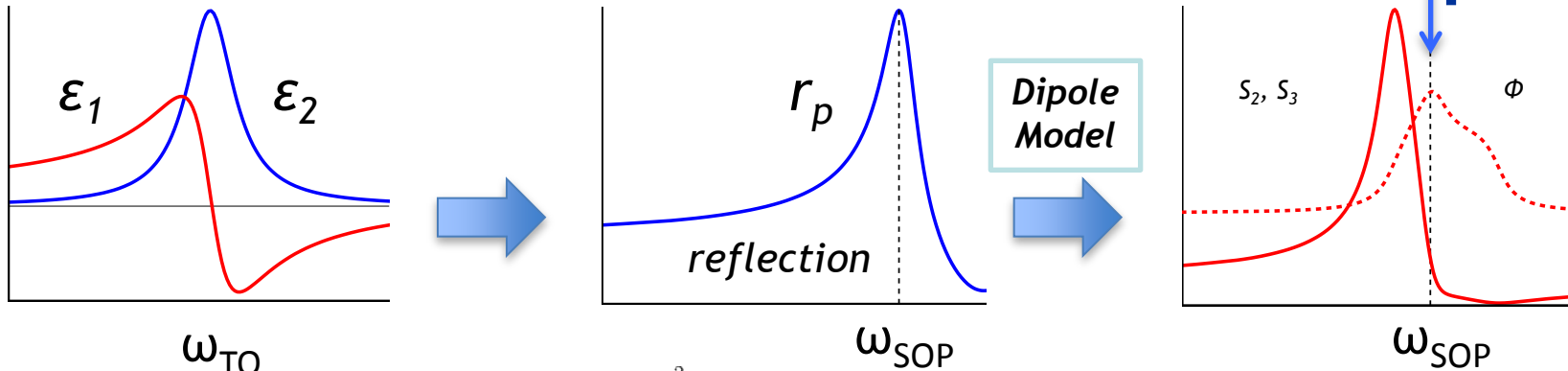
Near-Field IR Spectroscopy/Microscopy

Amarie, Keilmann, Phys Rev B **83**, 04504 (2011)



Near-field signal can be obtained within an integration time of 6.5 ms, which allows fast scan imaging (~150 pixels/s).

From Dielectric Function to Near-Field Response



$$R_p = \left| \frac{n_1 \cos \theta_t - n_2 \cos \theta_i}{n_1 \cos \theta_t + n_2 \cos \theta_i} \right|^2 = \left| \frac{n_1 \sqrt{1 - \left(\frac{n_1}{n_2} \sin \theta_i\right)^2} - n_2 \cos \theta_i}{n_1 \sqrt{1 - \left(\frac{n_1}{n_2} \sin \theta_i\right)^2} + n_2 \cos \theta_i} \right|^2$$

Fresnel equation for a single interface refraction

a – tip radius

α – polarizability of the tip apex

ϵ_t – dielectric function of the tip

ϵ_s – dielectric function of the sample

β – dielectric surface response function of the sample

α_{eff} – effective polarizability of the coupled tip-sample system

z – tip-sample distance

$\epsilon_{1,2}$ – Re and Im part of the dielectric function

ω_{TO} – transverse optical phonon frequency

ω_{SOP} – Surface optical phonon frequency

$S_{2,3}$ – Near field amplitude, 2nd, 3rd harmonic

Φ – optical field phase shift

$$\begin{aligned} d\lambda_{\text{nf}}(z) &= dE_s \frac{d\lambda_{\text{nf}}(z)}{dE_s} \\ &= dE_t \left(\mathcal{P}_{t \rightarrow s} \frac{dE_{\text{scat}}}{dE_{\text{inc}}} \Big|_s \mathcal{P}_{s \rightarrow t} \frac{d\lambda_{\text{nf}}(z)}{dE_{\text{scat}}} \right) \\ &= dQ_t \left(\frac{dE_t}{dQ_t} \mathcal{P}_{t \rightarrow s} \frac{dE_{\text{scat}}}{dE_{\text{inc}}} \Big|_s \mathcal{P}_{s \rightarrow t} \frac{d\lambda_{\text{nf}}(z)}{dE_{\text{scat}}} \right) \\ &= dQ_t \int_0^\infty dq \left(\frac{d}{dQ_t} \left(\frac{dE_{Q,t}}{dq} \right) \mathcal{P}_{t \rightarrow s}(q) \int_0^\infty dq' \frac{dE_{\text{scat},q'}}{dE_{\text{inc},q}} \Big|_s \mathcal{P}_{s \rightarrow t}(q') \frac{d\lambda_{\text{nf},q'}(z)}{dE_{\text{scat},q'}} \right) \\ &\equiv dQ_t \iint_0^\infty dq dq' \mathcal{G}(q) \mathcal{P}_{t \rightarrow s}(q) R(q, q') \mathcal{P}_{s \rightarrow t}(q') \Lambda(q', z) \end{aligned}$$

Alex McLeod Swinton. PhD thesis, 2013

$$\alpha = 4\pi a^3 \frac{\epsilon_t - 1}{\epsilon_t + 2}, \quad \beta = \frac{\epsilon_s - 1}{\epsilon_s + 1}$$

$$\alpha_{\text{eff}} = \frac{\alpha(1 + \beta)}{1 - \alpha\beta/(16\pi(a + z)^3)}$$